

MODELLING SUBSIDENCE IN GEOTHERMAL FIELDS

A. YEH AND M. J. O'SULLIVAN

Department of Engineering Science, University of Auckland, Auckland, New Zealand

SUMMARY - A three-dimensional subsidence modelling method is described here based on linking two computer codes: TOUGH2 and ABAQUS. TOUGH2 is a well-established finite volume code for simulating complex multi-phase multi-component sub-surface flows. It is widely used for geothermal reservoir modelling. ABAQUS is a general purpose finite element package that can be used for solving geotechnical problems. It can handle three-dimensional problems for heterogeneous materials with very general and complex constitutive properties. The pressure drop data available from the finite volume TOUGH2 model is converted into a body force distribution that causes deformation of the soil/rock structure. It is then interpolated on to the finite element mesh used for the ABAQUS rock mechanics calculation, which provides the surface deformation or subsidence. The conversion process between the two computational grids uses a least squares finite element method with smoothing to interpolate the pressure data from block centres in the TOUGH2 model to element vertices in the ABAQUS model. This process allows for the ABAQUS grid to be finer than the TOUGH2 grid. Results are presented for a simple test problem.

1. INTRODUCTION

Land subsidence associated with geothermal development has been observed and studied for decades in New Zealand. Several modelling studies have been carried out to help investigate the cause and to make future predictions. This paper introduces a new method of modelling geothermal subsidence, and in particular for the subsidence at the Wairakei-Tauhara geothermal field. The method could also easily be applied to other geothermal fields.

Subsidence is modelled three-dimensionally here using the ABAQUS code, with pressure changes directly input from three-dimensional reservoir flow model based on the TOUGH2 simulation.

The pressure change information from the TOUGH2 model is processed and passed into ABAQUS taking account of the difference between the computational meshes used in TOUGH2 and ABAQUS. The subsidence (surface deformation) is then calculated directly by ABAQUS.

1.1 Subsidence in the Wairakei-Tauhara Geothermal Field

The Wairakei and Tauhara geothermal fields are located to the north of Lake Taupo, at the centre of the North Island, New Zealand.

Subsidence was detected soon after the geothermal power plant started operation at Wairakei in 1950s. The subsidence rates in-

creasing from the 1950s to a peak in the 1970s, followed by decrease in rate down to approximately half the peak rate at present (Allis 2000). In the most intense subsidence area, the *Wairakei subsidence bowl* near the Eastern Borefield, the peak rate was 480 mm/year and has now slowed to a rate of 220 mm/year. The centre of the subsidence bowl has subsided a total of more than 15 m since the 1950s. The extent of the bowl where the subsidence rate is abnormally higher than surrounding areas is generally considered to be approximately 1 km². A slower subsidence rate between 5 and 100 mm/year has occurred over most of the Wairakei-Tauhara area.

The pressure of the deep Wairakei reservoir has dropped by around 25 bar since the development of the field in the 1950s (Allis 2000). Unlike the localised subsidence bowl, the area of pressure drawdown is wide-spread and reasonably uniform within the resistivity boundary, which encloses more than 20 km² in area. The deep reservoir pressure drawdown has also propagated to the Tauhara area.

1.2 Previous Works

Several techniques related to Geertsma's *one-dimensional compaction* and *subsidence/compaction relationship* were reviewed by Herd (1985). When the quantity of pressure decline is known or assumed (ie no flow simulation done), Geertsma's (analytical) nucleus-of-strain method provides the easiest way to calculate three-dimensional subsidence.

However, Geertsma's method approximates the region of interests as a linear elastic half-space, and this over-simplification and inflexibility is inappropriate for modelling the subsidence bowl in complex geothermal setting, such as Wairakei.

Herd used a finite element method to study two simple models, based on a two-layer two-dimensional cross-section of the Wairakei geothermal field. These two models were used to investigate whether the cause of the localised subsidence bowl was lateral variation in compressibility or lateral variation in pressure drawdown. However, no clear conclusion could be made because insufficient data was available and because of the overly simplified geometry and loading.

Allis (Allis and Zhan 2000, Allis 2004, Allis et al. 2001) has studied subsidence at Wairakei field for more than 15 years. He used Geertsma's techniques to try to identify the geological layer that contributes most to the subsidence bowl at Wairakei. Recently Allis used a one-dimensional finite-element model that couples compaction and fluid flow processes in porous materials to simulate the subsidence bowl at Wairakei. The code was originally developed by Lewis et al. (Lewis and Schrefler 1987, Schrefler and Zhan 1993). It has been used extensively on studies of subsidence induced by groundwater extraction around the northern Italian coast. Allis used it to set up one-dimensional models to match the levelling bench marks at Wairakei. Some good fits were obtained. However, the models are limited because they are only one-dimensional and some three-dimensional effects may be important at Wairakei (Terzaghi 2004, p. 15). Another limitation of Allis's modelling technique is that it allows for only single-phase flow. Thus the flow in the two-phase zones of Wairakei-Tauhara cannot be represented.

Terzaghi et al. (Lawless et al. 2001, Terzaghi 2004, White et al. 2005) have also developed models of subsidence at Wairakei by using a finite-element analysis software package, PLAXIS, that simulates coupled compaction and fluid flow. Several two-dimensional cross-sectioned models have been used to calculate the subsidence at both the Wairakei subsidence bowl and the more recent Tauhara subsidence bowl. However the Terzaghi models are limited because they are two-dimensional rather than three-dimensional. Also they cannot represent two-phase flow. Terzaghi (2004, p. 21) refers to the use of manually adjusted inputs to account for the effect of multiphase flows that are significant in the case of Wairakei geothermal

field and are not accounted for in the PLAXIS code.

All of these models give results that agree reasonably well with past subsidence history along the selected points or cross-section lines. However, the different studies disagree about the cause of the severe subsidence, especially at the Wairakei subsidence bowl. It is hoped that the three-dimensional model developed in the current research can simulate subsidence more completely over the whole geothermal area, making future predictions more reliable.

1.3 Modelling Software

Two software packages are used in a linked manner in the current study of subsidence in geothermal fields:

- TOUGH2 (Pruess et al. 1999) is a simulator for flows of multi-component and multi-phase fluids in porous medium. It has been used widely for geothermal reservoir modelling, in fields such as Wairakei-Tauhara (Mannington et al. 2004).
- ABAQUS (2003) is a general purpose finite element code that is generally used to solve stress-strain problems. It supports a large number of material constitutive behaviour. It can solve one-, two-, or three-dimensional problems.

Modelling subsidence in other geothermal fields where TOUGH2 is used for reservoir modelling could also be easily performed using our linked approach. Ohaaki geothermal field (New Zealand), where subsidence is also occurring, is an example.

2. SOLUTION TECHNIQUE

The subsidence modelling approach here is uncoupled: the mass and energy transport geothermal model is separate from the solid deformation of subsidence model. Pressure changes from the TOUGH2 flow model are converted into body force that acts on the soil/rock structure of the ABAQUS solid model. Subsidence is then calculated from the deformation of the ABAQUS model.

A previous work by Rutqvist et al. (Rutqvist et al. 2002, Rutqvist and Tsang 2003) is carried out in a similar fashion. A staggered and lagged procedures is adapted for solving coupled thermal-hydrologic-mechanical problems, such as disposal of nuclear waste in unsatu-

rated fractured porous media. This is a partially coupled method because permeabilities and porosities are adjusted. This is slightly different from the uncoupled method described in the present paper. The TOUGH2 code was linked with FLAC3D, a commercial code that is designed for rock and soil mechanics.

2.1 Uncoupled Modelling

The assumption of weak coupling between the stress and flow field leads to the development of an uncoupled method here. It is reasonable to assume that the long-term regional scale subsidence generally causes slow and small changes in permeability and porosity. The effects of these changes will not play a significant role in the large scale flow simulation carried out with TOUGH2. Hence the information passed from the flow model to the solid deformation model is one-way.

It is also easier to adapt two computer codes that are known to perform well in each field rather than finding or developing one computer code that can simulate a complicated coupled problem. This is especially true in geothermal subsidence modelling, because geothermal reservoir modelling involves very complicated heat and mass transfer processes, which cannot be modelled with existing stress-strain-fluid flow simulators such as PLAXIS.

Furthermore, the ability to utilise well-established reservoir models is an advantage. TOUGH2 has been used extensively to model geothermal reservoirs. This is especially true for the Wairakei-Tauhara geothermal field. The University of Auckland TOUGH2 model for Wairakei-Tauhara (Mannington et al. 2004) is well-recognised. Future scenarios have been carried out to predict reservoir state in the future. This makes the prediction of the subsidence possible with our technique.

Calibration of two separate models is generally considered easier than one single coupled model, especially the causal interaction is stronger one way than the other. The advantage of using TOUGH2 reservoir model is apparent here: models like Wairakei-Tauhara has been constantly improved and are likely to be further improved in the future. All improvement made on the TOUGH2 model will benefit the solid deformation model.

2.2 Pressure-Body Force Conversion

The conversion of pressure change data from TOUGH2 to a body force field that drives the ABAQUS model is described here.

In a fluid saturated porous medium, the components of stress satisfy the following equilibrium equations:

$$\begin{aligned}\frac{\partial \sigma_{xx}}{\partial x} + \frac{\partial \sigma_{xy}}{\partial y} + \frac{\partial \sigma_{xz}}{\partial z} &= 0 \\ \frac{\partial \sigma_{xy}}{\partial x} + \frac{\partial \sigma_{yy}}{\partial y} + \frac{\partial \sigma_{yz}}{\partial z} &= 0 \\ \frac{\partial \sigma_{xz}}{\partial x} + \frac{\partial \sigma_{yz}}{\partial y} + \frac{\partial \sigma_{zz}}{\partial z} + \rho g &= 0.\end{aligned}\quad (1)$$

Here ρ is density of the fluid saturated bulk rock, and g is the acceleration due to gravity.

Based on the soil mechanics concept of Terzaghi (Biot 1941), the total stress σ_{ij} is composed of the effective stress and the pore pressure. Effective stress, denoted by σ_{ij}^* , is the stress which acts on the solid structure of the rock. The pore pressure P is the fluid pressure within the pores of the rock. Using ϕ to represent the porosity of the rock, the three normal stress components can be rewritten as follows (Biot 1956):

$$\begin{aligned}\sigma_{xx} &= \sigma_{xx}^* - \phi P \\ \sigma_{yy} &= \sigma_{yy}^* - \phi P \\ \sigma_{zz} &= \sigma_{zz}^* - \phi P.\end{aligned}\quad (2)$$

Here the sign of the pressure term is negative, following the normal convention of taking tensile stress as positive.

Fluid in the pores is considered to have no ability to sustain shear force. Hence, the total shear stresses are equal to the corresponding effective shear stresses:

$$\begin{aligned}\sigma_{xy} &= \sigma_{xy}^* \\ \sigma_{yz} &= \sigma_{yz}^* \\ \sigma_{xz} &= \sigma_{xz}^*.\end{aligned}\quad (3)$$

Using equations (2) and (3), then (1) can be rewritten as:

$$\begin{aligned}\frac{\partial(\sigma_{xx}^* - \phi P)}{\partial x} + \frac{\partial \sigma_{xy}^*}{\partial y} + \frac{\partial \sigma_{xz}^*}{\partial z} &= 0 \\ \frac{\partial \sigma_{xy}^*}{\partial x} + \frac{\partial(\sigma_{yy}^* - \phi P)}{\partial y} + \frac{\partial \sigma_{yz}^*}{\partial z} &= 0 \\ \frac{\partial \sigma_{xz}^*}{\partial x} + \frac{\partial \sigma_{yz}^*}{\partial y} + \frac{\partial(\sigma_{zz}^* - \phi P)}{\partial z} + \rho g &= 0.\end{aligned}\quad (4)$$

The above equilibrium equations are useful for scenarios where the fluid pressure changes slowly over time and the short-term transient effects are small. In this case subsidence is calculated as a sequence of quasi-equilibrium

problems. Writing the initial fluid pressure as P_0 , and the final fluid pressure as P_1 , their difference can be represented by a function $f(x, y, z)$:

$$P_1 = P_0 + f. \quad (5)$$

By expressing two sets of equilibrium equations (4) using P_0 and P_1 , and subtracting, the difference between initial and final states can be obtained in the form:

$$\begin{aligned} \frac{\partial \overline{\sigma_{xx}^*}}{\partial x} + \frac{\partial \overline{\sigma_{xy}^*}}{\partial y} + \frac{\partial \overline{\sigma_{xz}^*}}{\partial z} + \frac{\partial}{\partial x}(-\phi f) &= 0 \\ \frac{\partial \overline{\sigma_{xy}^*}}{\partial x} + \frac{\partial \overline{\sigma_{yy}^*}}{\partial y} + \frac{\partial \overline{\sigma_{yz}^*}}{\partial z} + \frac{\partial}{\partial y}(-\phi f) &= 0 \\ \frac{\partial \overline{\sigma_{xz}^*}}{\partial x} + \frac{\partial \overline{\sigma_{yz}^*}}{\partial y} + \frac{\partial \overline{\sigma_{zz}^*}}{\partial z} + \frac{\partial}{\partial z}(-\phi f) + \overline{\rho g} &= 0, \end{aligned} \quad (6)$$

where $\overline{\sigma^*}$ is the difference in effective stress. Here $\overline{\rho} = \rho_1 - \rho_0$ where ρ_1 and ρ_0 are the final and initial density of the fluid saturated bulk rock. If the change in density of the rock solid skeleton ($\overline{\rho_s}$) is assumed to be negligible, then change of density can be calculated directly by using the density change of fluid alone, that is:

$$\begin{aligned} \overline{\rho} &= \phi \overline{\rho_f} + (1 - \phi) \overline{\rho_s} \\ &\approx \phi \overline{\rho_f}. \end{aligned} \quad (7)$$

In a liquid-vapour two phase system, fluid density can be calculated from densities of each phase:

$$\rho_f = \rho_l S_l + \rho_v S_v, \quad (8)$$

where ρ_l and S_l are density and saturation of liquid phase; ρ_v and S_v are density and saturation of vapour phase.

These *incremental equilibrium equations* (6) are very useful. By comparison to the general stress equilibrium equations (1), it is obvious that the only difference is in the introduction of effective body force terms given by $\partial(-\phi f)/\partial x$, $\partial(-\phi f)/\partial y$, and $\partial(-\phi f)/\partial z + \overline{\rho g}$ in the x , y , z directions, respectively.

Once (6) is solved for the increment in stress, the the small changes in strain (deformation), $\delta\varepsilon$, can be calculated from small changes in stress, $\delta\sigma$, which is induced by the applied body force, by using the simple stress-strain relation (Lewis and Schrefler 1987, p. 99):

$$\delta\varepsilon = \mathbf{D}\delta\sigma \quad (9)$$

where \mathbf{D} , represents the material constants. For a simple elastic isotropic material, the number of independent components of \mathbf{D} can reduce from 21 to 2. However, more complex material behaviours are also possible.

In the present research, $\nabla(-\phi f)$ is used as the body force in the ABAQUS stress-strain analysis, without the effect of $\overline{\rho g}$, which makes a smaller contribution to the overall subsidence. The density term $\overline{\rho g}$ could be added into the body force in future work.

2.3 Linking Tough2 and Abaqus

TOUGH2 is used to model the mass and energy transport, while ABAQUS is responsible to solve the solid deformation problem. This project develops the interface software that connects these two totally different software packages. Two main processes are involved in this software: mesh conversion and data conversion (from pressure change to body force field).

The finite volume method used by TOUGH2 has field variables, such as pressure and temperature, in each block. ('Block' is the term selected here for TOUGH2's computational unit, in order to distinguish from ABAQUS's 'element'.) The variables are defined at the centres of the blocks that represent the block averaged quantities.

The finite element method used by ABAQUS has the field variables stored at the nodes of elements. Neighbouring elements share field variables stored at their common nodes.

The fact that TOUGH2's finite volume method and ABAQUS's finite element method are different in nature leads to complexity in both mesh and data conversion.

Mesh Conversion - In general, it is not necessary to have related meshes for both TOUGH2 and ABAQUS models. It is, however, advantageous to have grids which share a common structure. The ABAQUS model could be readily updated with improvements made to the TOUGH2 mesh if the mesh is directed converted. Both the flow model and the subsidence model should have a fine grid in areas where pressure changes are large.

Unlike finite elements, there is virtually no rules for creating a finite volume mesh. This makes the direct conversion, 'direct block to element' where block/element boundaries coincident, complicated. The TOUGH2 mesh could have blocks with shapes that cannot be used in ABAQUS's finite element mesh.

For example TOUGH2 allows more than one neighboring blocks to be connected to the single face of a larger block. This type of mesh

refinement is often used at the interface between fine and coarse grid regions, but finite elements do not allow this. An automated code was developed to divide such interface blocks into two or more blocks that follow the finite element rules.

Data Conversion - The body force term which is applied to the finite element deformation model is the spatial derivative $\nabla(-\phi f)$. The value of total pressure decrease multiplied by porosity, $-\phi f$, provided at the centre of each TOUGH2 block must be approximated by a continuous spatial function. Then the gradient/derivative of this function can be calculated. It is natural to fit the pressure data to a finite element mesh that is used directly by ABAQUS. One of the most common techniques serving this purpose is *least squares finite-element fitting*.

The ABAQUS mesh here is generally required to be at least the same and often finer than the mesh used by the TOUGH2 model in order to obtain enough subsidence information. This is due to the fact that reservoir models usually have relatively large scale, more than 10 kilometres wide and a few km deep, while the subsidence magnitude and region we are looking at may be small, such as 1 km² area with maximum of 15 m deformation. This introduces the problem of interpolating pressure data from a coarse TOUGH2 grid on to a finer ABAQUS grid.

It is well-recognised that insufficient sampled data may cause the least squares finite element fitting to break down. Regularisation must be performed in order to obtain a meaningful solution. The finite element data fitting method with a smoothness constraint was adopted by Young (Young 1990, Young et al. 1992), for fitting coronary data sets to a finite element mesh of a epicardial surface, and Croucher (Croucher 1998), for fitting measured water depths to a finite element mesh for analysis of tidal flows in shallow water. In both of these cases, the technique was used successfully to deal with scattered data. This *least squares finite element fitting with smoothing* is described very briefly here.

In a simple least squares finite element fitting, the residual, denoted by $P(u)$ here, is required to be minimised in this problem:

$$P(u) = \sum_{d=1}^D (u(x_d) - u_d)^2 \quad (10)$$

where u is the scalar field of $(-\phi f)$ that we are trying to fit onto our finite element mesh, $u_d, d = 1 \dots D$ is the sampled data values at po-

sitions $x_d, d = 1 \dots D$, where D is number of data values. Function $P(u)$ is the discrepancy between the sampled data and fitted function which measures the fidelity of the approximation.

Regularisation could be performed by imposing additional constraints on the fitting field value. Terzopolous (1986) developed a generalised approximation error function with regularisation on smoothness:

$$\varepsilon(u) = S(u) + P(u) \quad (11)$$

where $S(u)$ measures the smoothness of the approximation. This new error function $\varepsilon(u)$ is to be minimised by the same way as normal finite element fitting.

The smoothness control term $S(u)$ introduced by Terzopolous is in the form of a generalised *controlled-continuity stabiliser*:

$$S(u, p, w) = \sum_{m=0}^p \int_{\mathbb{R}^d} w_m(x) \times \sum_{\substack{j_1+\dots \\ +j_d=m}} \frac{m!}{j_1! \dots j_d!} \left(\frac{\partial^m u(x)}{\partial x_1^{j_1} \dots \partial x_d^{j_d}} \right)^2 dx. \quad (12)$$

Using specified values from Young (1990), $p = 2$, $w_0 = 0$, $w_1 = \alpha$, $w_2 = \beta$, stabiliser S now controls the smoothness with two positive *smoothing parameters* α and β . Here α limits the gradients, β controls the curvatures of the *value surface* on the faces of the elements. Since our case is three-dimensional, Eqn. (12) becomes:

$$S(u) = \int_{\Omega} \left\{ \alpha \left[\left(\frac{\partial u}{\partial x_1} \right)^2 + \left(\frac{\partial u}{\partial x_2} \right)^2 + \left(\frac{\partial u}{\partial x_3} \right)^2 \right] + \beta \left[\left(\frac{\partial^2 u}{\partial x_1^2} \right)^2 + \left(\frac{\partial^2 u}{\partial x_2^2} \right)^2 + \left(\frac{\partial^2 u}{\partial x_3^2} \right)^2 + 2 \left(\frac{\partial^2 u}{\partial x_1 \partial x_2} \right)^2 + 2 \left(\frac{\partial^2 u}{\partial x_1 \partial x_3} \right)^2 + 2 \left(\frac{\partial^2 u}{\partial x_2 \partial x_3} \right)^2 \right] \right\} dx_1 dx_2 dx_3 \quad (13)$$

where the Ω is the model domain.

The smoothness parameters α and β are positive real numbers that control the gradients of the approximated values and the curvature of the ‘value surface’ on faces of the element. As α and β increase, the smoother the solution becomes. When α and β reduce to zero, the algorithm is identical to the least squares finite element fitting without regularisation/smoothing.

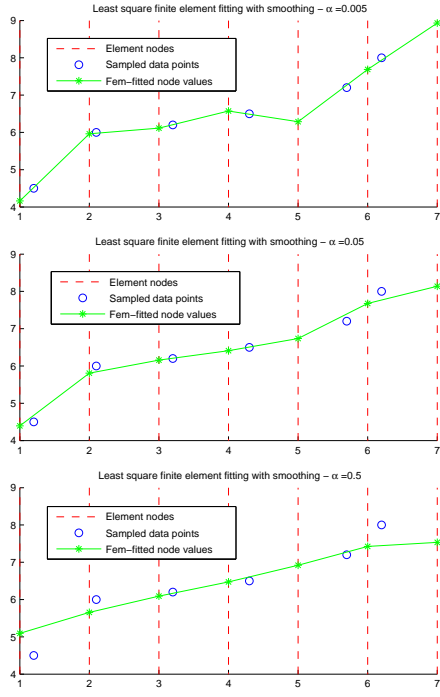


Figure 1 - Comparison of fitted results with different smoothing parameters

An example of the smoothing effect is shown in Figure 1. This is a one-dimensional case, where there is no curvature control term. The parameter α is varied to show the effect of smoothing on the fitted solution. Clearly, as we increase the size of α , the accuracy of the approximation is lost.

It is important to realise that the optimal size of these parameters strongly depends on the mesh. The optimal values of α and β cannot be determined before running actual tests on the problem at hand. The most common method is to carry out a series of numerical experiments and select the results that adequately represents the sampled data field with acceptable smoothness. A more systematic way of optimising the smoothing parameters is to use the well-known method of L-curves (Hansen 1992) which finds the set of parameters that balances smoothness and fidelity.

3. A SIMPLE TWO-DIMENSIONAL TEST CASE

A test case is presented here for modelling subsidence caused by producing fluid at depth. The reservoir TOUGH2 model was set up with $100 \times 100 \times 1$ blocks. All blocks have the same properties, and are identical, $10 \text{ m} \times 10 \text{ m} \times 100\text{m}$ thick. Constant atmospheric temperature is assumed for the whole reservoir, hence the problem is isothermal and single-phase. A

single production well is placed at the centre of the model with a constant production rate. The pressure at natural state and final state after production is shown in Fig. 2. There is a significant pressure drop at the centre.

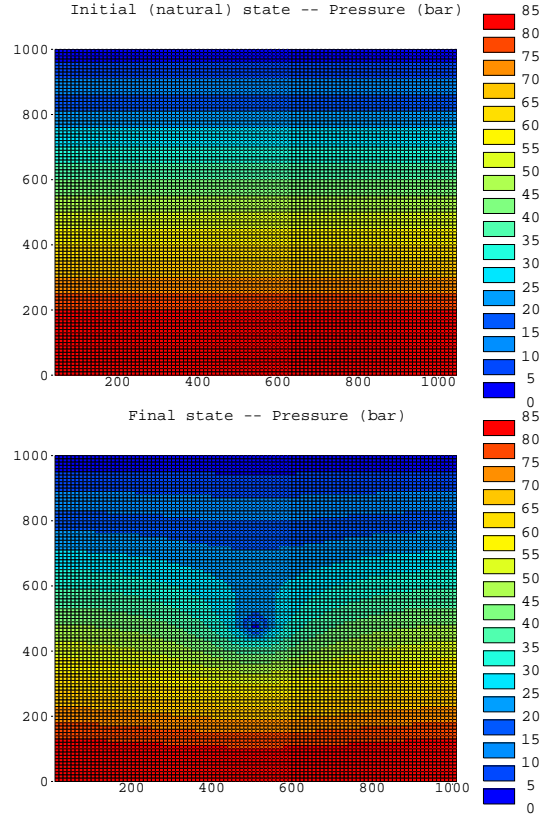


Figure 2 - Pressure field of the initial state (upper) and final state (lower)

The difference between those two states is represented by the f value. All f values are then multiplied by $-\phi$, negative porosity, which is a constant in this case. The gradients $\partial(-\phi f)/\partial x$ and $\partial(-\phi f)/\partial y$ are calculated by finite difference approximations (convenient for regular mesh like the case here). Body force terms in two directions ($\partial(-\phi f)/\partial x$ and $\partial(-\phi f)/\partial y$) were applied as constant values over the area of each element.

The plane strain option in ABAQUS is used. The solid mechanics boundary conditions applied for these test cases are shown in Fig. 3

Here the simplest material model is used, that is the linear isotropic elastic option (ABAQUS Inc. 2003, p. 10.2.1-2). This material is assigned uniformly to the whole model.

The solid deformation simulations were carried out at the end of the flow calculation with f calculated from the pressure change between the original ($t = 0$) state and the current state. All solutions shown here are for the final state

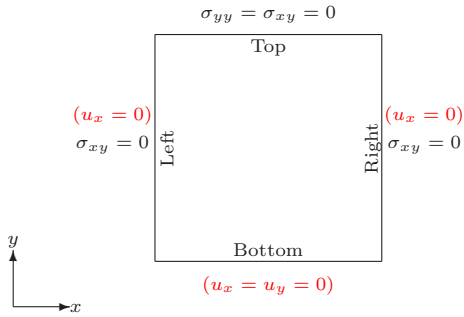


Figure 3 - Boundary conditions applied in ABAQUS

after a certain time of production.

Fig. 4 illustrate the displacement of nodes in directions y (U2). The contraction within the well withdrawal area (centre) can be clearly observed. Nodes above the central area show significant negative U2 value. The deformation scale factor is 300.

The most important and most direct impact of subsidence effects is seen in the surface movement. The vectors in Fig. 5 show the direction of movement for each of the nodes (only surface nodes are shown here). The shape clearly reveals the curvature of the expected 'subsidence bowl'. The vectors show both vertical and horizontal movement in the subsidence bowl.

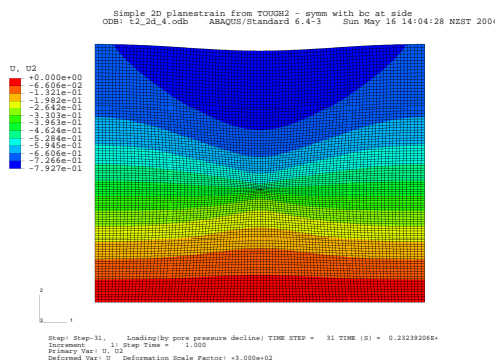


Figure 4 - Displacement in y direction, simple regular mesh model

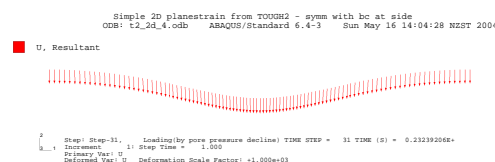


Figure 5 - Surface subsidence, simple regular mesh model

4. DISCUSSION

4.1 Calibration

This paper only attempts to illustrate the method and to show that it can work. More effort is required to carefully calibrate/validate models to match real subsidence data. This could be achieved by improving three different aspects of the model: better pressure matches in flow model, suitable smoothing parameters for pressure-body force conversion, and calibration of material properties in the solid deformation model.

Pressure decline is one of the prime factors that is known to affect greatly the final subsidence. It is important to have a well-calibrated TOUGH2 flow model based on good pressure information. It is also important to carefully calibrate the pressure, especially the shallow (within 500 metres depth) pressure near areas of interest, which are generally considered to be the main compaction zones.

The selection of smoothing parameters could be achieved by running a series of trial runs, varying parameters, then choosing those that capture the fidelity of the pressure decline with sufficient smoothing. This must be checked every time a different mesh is used, either in the TOUGH2 or ABAQUS model.

Material properties are also the most important parameters. Parameters should be chosen with some knowledge of the geology and measured rock properties. Different material types, such as plastic properties should also be considered to allow for more realistic soil/rock behaviour.

4.2 Boundary Conditions

Precautions must be taken with the boundary conditions when the method in this paper is applied. It is important to realise that the body force, converted from the pressure change, is only the change in effective stress. It is the difference between the initial and the end state. If the pressures on the boundaries change, then the boundary conditions applied to the solid deformation model should also reflect the changes.

An example is modelling a small region of *uniform pressure decline*, within a large model. The pressure change (f) is a constant throughout the whole model. Assuming constant porosity (ϕ), the converted body force

$(\nabla(-\phi f))$ will be zero. This does not, however, imply that there is no deformation as a result. Note that the conditions at the boundaries have changed with a constant pressure drop. This must be reflected by changing the pressure on the boundaries in the solid deformation model, which *will* cause change in stress and hence a deformation, as intuitively predicted.

5. CONCLUSIONS

The coupled phenomenon of subsidence in geothermal fields involves mechanisms of both fluid flow and solid deformation. The weak coupling between them in the case of long-term large scale subsidence enables the uncoupled method to produce reasonable solutions.

This paper proposes a method that systematically links TOUGH2 and ABAQUS together, by converting the pressure changes in the fluid flow model into the body force that deforms the soil/rock in the solid deformation model. Based on Biot's original coupled consolidation theory, the body force is obtained by computing the gradients of the total pressure changes between the initial and current state. This body force represents the stress difference between these two states. Then it can be applied to the solid deformation model with any suitable material properties. Both the TOUGH2 fluid flow model and ABAQUS solid deformation model can be three-dimensional.

Calibration of the flow and subsidence models can be improved in three respects: improving the pressure in reservoir model, selecting smoothing parameters, and calibrating material properties in the solid deformation model.

A simple two-dimensional test case is used to demonstrate the method here. The subsidence caused by fluid withdrawal in a TOUGH2 model is successfully simulated in ABAQUS. Work is progressing on applying this method to model the subsidence in the Wairakei-Tauhara geothermal fields.

6. ACKNOWLEDGEMENTS

Thanks to Contact Energy Ltd., for funding this project under a UniServices/Contact Energy research contract.

7. REFERENCES

ABAQUS Inc. (2003). *ABAQUS Analysis User's Manual Version 6.4*, ABAQUS Inc., Pawtucket, RI.

Allis, R., Clotworthy, A., Currie, S. and Zhan, X. (2001). Update of subsidence of Wairakei-Tauhara geothermal system, *Proceeding 23rd NZ Geothermal Workshop 2001*, pp. 91–97.

Allis, R. G. (2000). Review of subsidence at Wairakei field, New Zealand, *Geothermics* Vol. 29, 455–478.

Allis, R. G. (2004). In the matter of the Resource Management Act 1991 and in the matter of an application by Contact Energy Limited for resource consents for the Wairakei Geothermal Power Plant. New Zealand.

Allis, R. G. and Zhan, X. (2000). Predicting subsidence at Wairakei and Ohaaki geothermal fields, New Zealand, *Geothermics* Vol. 29, 479–497.

Biot, M. A. (1941). General theory of three dimensional consolidation, *Journal of Applied Physics* Vol. 12, 155–165.

Biot, M. A. (1956). General solutions of the equations of elasticity and consolidation for a porous material, *Journal of Applied Mechanics* Vol. 23, 91–96.

Croucher, A. E. (1998). *Modelling contaminant transport in rivers and estuaries*, Ph.D. Thesis, University of Auckland, New Zealand.

Hansen, P. C. (1992). Analysis of discrete ill-posed problems by means of the L-curve, *Society for Industrial and Applied Mathematics* Vol. 34(4), 561–580.

Herd, M. A. (1985). *Mathematical modelling of subsidence above geothermal reservoirs*, M.E. Thesis, University of Auckland, New Zealand.

Lawless, J. V., Okada, W., Terzaghi, S. and White, P. J. (2001). New 2-D subsidence modelling applied to Wairakei-Tauhara, *Proceeding 23rd NZ Geothermal Workshop 2001*, pp. 105–111.

Lewis, R. W. and Schrefler, B. A. (1987). *The Finite-Element Method in the Deformation and Consolidation of Porous Media*, Wiley, Chichester, England.

Mannington, W. I., O'Sullivan, M. J., Bullivant, D. P. and Clotworthy, A. W. (2004). Reinjection at Wairakei-Tauhara: a modelling case study, *Twenty-Ninth Workshop on Geothermal Reservoir Engineering*, Stanford University, Stanford, California.

Pruess, K., Oldenburg, C. and Moridis, G. (1999). *TOUGH2 User's Guide Version 2.0*, University of California, Berkeley, California, USA.

Rutqvist, J. and Tsang, C. F. (2003). TOUGH-FLAC: a numerical simulator for analysis of coupled thermo-hydrologic-mechanical processes in fractured and porous geological media under multi-phase flow conditions, *TOUGH Symposium 2003*, Lawrence Berkeley National Laboratory, Berkely, California.

Rutqvist, J., Wu, Y. S., Tsang, C. F. and Bodvarsson, G. (2002). A modeling approach for analysis of coupled multiphase fluid flow, heat transfer, and deformation in fractured rock, *International Journal of Rock Mechanics & Mining Science* Vol. 39, 429–442.

Schrefler, B. A. and Zhan, X. (1993). A fully coupled model for water flow and airflow in deformable porous media, *Water Resources Research* Vol. 29, 155–167.

Terzaghi, S. (2004). In the matter of the Resource Management Act 1991 and in the matter of a hearing by Waikato Regional Council of a submission by Taupo District Council in relation to applications by Contact Energy Limited for the resource consents required for activities related to the use of the Wairakei-Tauhara geothermal system for electricity generation purposes. New Zealand.

Terzopoulos, D. (1986). Regularization of inverse visual problems involving discontinuities, *IEEE Transactions on Pattern Analysis and Machine Intelligence* Vol. 8(4), 413–424.

White, P. J., Lawless, J. V., Terzaghi, S. and Okada, W. (2005). Advances in subsidence modelling of exploited geothermal fields, *Proceedings World Geothermal Congress 2005*.

Young, A. A. (1990). *Epicardial deformation from coronary cinéangiograms*, Ph.D. Thesis, University of Auckland, New Zealand.

Young, A. A., Hunter, P. J. and Smaill, B. H. (1992). Estimation of epicardial strain using the motions of coronary bifurcations in biplane cinéangiography, *IEEE Transactions on Biomedical Engineering* Vol. 39(5), 526–531.